Atmos. Chem. Phys. Discuss., 10, 10589–10623, 2010
www.atmos-chem-phys-discuss.net/10/10589/2010/

Atmospheric Chemistry and Physics Discussions

This discussion paper is/has been under review for the journal Atmospheric Chemistry and Physics (ACP). Please refer to the corresponding final paper in ACP if available.

Direct observation of aerosol particles in aged agricultural biomass burning plumes impacting urban atmospheres

W. Y. Li[1,2,3] **and L. Y. Shao**[2]

[1]Environment Research Institute, Shandong University, Jinan, Shandong 250100, China
[2]State Key Laboratory of Coal Resources and Safe Mining & College of Geoscience and Surveying Engineering, China University of Mining and Technology, Beijing 100083, China
[3]School of Earth and Space Exploration and Department of Chemistry and Biochemistry, Arizona State University, Tempe, AZ 85287-1404, USA

Received: 26 January 2010 – Accepted: 20 April 2010 – Published: 22 April 2010

Correspondence to: L. Y. Shao (shaol@cumtb.edu.cn)

Published by Copernicus Publications on behalf of the European Geosciences Union.

Abstract

Emissions from agricultural biomass burning (ABB) in northern China have a significant impact on the regional and the global climate. According to the Giovanni's Aerosol optical depth (AOD) map, the monthly average AOD at 550 nm in northern China in 2007 shows a maximum value of 0.7 in June, suggesting that episodes of severe aerosol pollution occurred in this region. Aerosol particles were collected in urban Beijing during regional brown hazes from 12 to 30 June, 2007. Transmission electron microscopy with energy-dispersive X-ray spectrometry characterized the morphology, composition, and mixing state of aerosol particles. Potassium salts (K_2SO_4 and KNO_3), ammonium sulfate, soot, and organic particles predominated in fine particles (diameter <1 μm) collected from 12 to 20 June, 2007. In contrast, from 21 to 30 June, 2007, ammonium sulfate, soot, and organic particles were dominant. Potassium-dominant particles as a tracer of biomass burning, together with wildfire maps, show that intensive regional ABB in northern China from 10 to 20 June, 2007 contributed significantly to the regional haze. After long-range transport, ABB particles exhibited marked changes in their morphology, elemental composition, and mixing state. Heterogeneous reactions completely converted KCl particles from ABB into K_2SO_4 and KNO_3. Soot particles were generally mixed with potassium salts, ammonium salts, and organic particles. In addition, the abundant aged organic particles and soluble salts emitted by ABB become more hygroscopic and increase their size during long-range transport, becoming in effect additional cloud condensation nuclei. The high AOD (average value at 2.2) during 12 to 20 June, 2007, in Beijing is partly explained by the hygroscopic growth of aged fine aerosol particles and by the strong absorption of internally mixed soot particles, both coming from regional ABB emissions.

ACPD

10, 10589–10623, 2010

1 Introduction

Biomass burning is a global phenomenon. It can release large quantities of atmospheric gases and aerosol particles which affect the atmospheric chemistry and climate directly by scattering and absorbing solar radiation on regional and global scales (Crutzen and Andreae, 1990). Moreover, aerosol particles from biomass burning dramatically increase cloud condensation nuclei (CCN) concentrations and affect the formation and lifetime of clouds (Andreae et al., 2004; Roberts et al., 2003). Such aerosol particles serving as CCN also indirectly alter the radiation budget of clouds in the troposphere (IPCC, 2007). In addition, because of the transport of biomass burning aerosols out of biomass regions and into urban areas, these aerosols alter the biogeochemical cycling and adversely affect human health (Bowman et al., 2009; Crutzen and Andreae, 1990; Da Rocha et al., 2005; Koe et al., 2001; Niemi et al., 2005; Reid et al., 2005). Agricultural biomass burning (ABB) activities in Asia are drawing worldwide attention to the rapidly developing China with its ever increasing agricultural activity. Numerous studies have shown that the mixtures of pollutants from industries, biomass burning, and urban areas in northern China can be transported over the Pacific Ocean (Jacob et al., 2003; Ma et al., 2003) into North America (de Gouw et al., 2004; Jaffe et al., 1999; Peltier et al., 2008; Yienger et al., 2000).

Compared with plumes from industrial and soil dust emissions, as well as with relatively clean air plumes, the plumes over northern China that contain emissions from biomass burning can show markedly distinct optical properties (Yang et al., 2009). In particular, massive quantities of fine soot particles (also known as black carbon or elemental carbon) from biomass burning are emitted into the troposphere. Ramanathan and Carmichael (2008) stress that soot in the troposphere is the second greatest contributor to global warming, behind carbon dioxide. In the atmosphere soot particles acquire coatings of sulfates, organic materials, and sulfuric acid (Adachi and Buseck, 2008; Johnson et al., 2005; Posfai et al., 1999). Such mixtures enhance the light absorption of soot particles above that of pure soot (Chung and Seinfeld, 2002; Jacobson,

ACPD
10, 10589–10623, 2010

2001; Lesins et al., 2002; Zhang et al., 2008). For example, sulfate-coated soot particles absorb 30% more light than soot alone (Fuller et al., 1999). Clearly, a complete physical and chemical investigation of ambient ABB aerosol particles, most particularly soot particles, must be conducted before climatic impacts of aerosols can be predicted in China.

In recent studies of ABB in China, Cao et al. (2008) estimated that ABB emissions from crop straw burning amount to 140 Tg/year; Duan et al. (2004) found that monthly average concentrations of K^+ in Beijing were three times higher in June than in May likely because of the ABB emissions; Zhang et al. (2007) showed that ABB emissions increased organic carbon (OC) and elemental carbon (EC) concentrations and that burning status significantly influenced the formation of EC and polycyclic aromatic hydrocarbons (PAHs). These studies, however, did not specifically evaluate the composition and mixing state of aged ABB aerosol particles in urban regions and their impacts on regional climate. Two reasons may explain this shortcoming. First, ABB emissions occur at different times within the spring season because the timing of farming activities changes from south to north in China, necessitating that more flexible sampling schedules need to be designed. Second, the frequent episodes of severe pollution with high mass concentrations of particulate matter (PM) from industrial and vehicular emission in urban areas may mask ABB aerosols in some cities, suggesting that the traditional bulk analytical methods cannot adequately characterize them. Therefore, the common bulk methods, which focus on the chemical composition of aerosol particle mass obtained from fairly long sampling durations, are unable to explicitly characterize ABB particles in those episodes. In addition, bulk methods only provide information about aerosol mixtures, not individual ABB particles.

In contrast, individual particle analysis with transmission electron microscopy (TEM) provides detailed information on individual particles at a high resolution (Buseck and Posfai, 1999). TEM is uniquely suited to observe and analyze the morphology, size, structure, and mixing state of individual fine atmospheric aerosol particles (Johnson et al., 2005; Posfai et al., 1999; Li and Shao, 2009a). Furthermore, TEM can detect

ACPD
10, 10589–10623, 2010

the presence of abundant potassium salts in biomass plumes and provide information about mixing states and aging processes of individual biomass burning particles (Adachi and Buseck, 2008; Posfai et al., 2003). In addition, particle collection for individual particle analysis requires a short sampling time, which means that unique pollution episodes with high temporal variability can be studied successfully.

In the present work, our goal is to understand properties of individual ABB particles that comprise a portion of the regional brown hazes in northern China. First, potassium-dominant aerosol particles are a tracer of biomass burning and, together with wildfire maps, can identify a regionally intense ABB source in the hazes that are formed by different anthropogenic and natural sources. Second, we observed mass concentrations of PM containing ABB aerosols in Beijing. With TEM particular attention was paid to the phase and mixing state of individual aerosol particles. Backward air mass trajectories, fire satellite observations, and aerosol optical depth (AOD) measurements from sun photometers were used to evaluate the effects of ABB-related aerosol particles in the brown hazes.

2 Materials and methods

2.1 Aerosol sampling

Aerosols were collected in seven haze episodes during 12–27 June, 2007 in northwestern urban Beijing (39°59′ N, 116°20′ E) (Table 1). With the samplers mounted 18 m above ground on the roof of a building on the campus of China University of Mining and Technology, aerosol particles were collected onto copper TEM grids coated with carbon film (carbon type B, 300-mesh copper) using a single-stage cascade impactor with a 0.5-mm-diameter jet nozzle with a flow rate of 1.0 l min^{-1}. This sampler has a collection efficiency of 100% at 0.5 µm aerodynamic diameter if the density of the particles is 2 g cm^{-3}. Sampling times varied from 30 to 120 s, depending on the visibility. Measurements of wind speed (WS), wind direction (WD), relative humidity (RH),

ACPD
10, 10589–10623, 2010

barometric pressure (P), and ambient temperature (T) were automatically recorded by a Kestral 4000 (Table 1). After collection, each sample was placed in a sealed dry plastic tube and was stored in a desiccator at 25° and 20±3% RH to preserve them for analysis and minimize their exposure to ambient air.

2.2 Generation of K_2SO_4 and KNO_3 particles in the laboratory

Aerosols particles of K_2SO_4 and KNO_3 were generated from 1 M solutions prepared from analytical reagent-grade chemicals (97% purity, Aldrich). The aerosols were dried using a silicon diffusion drier (TSI Model 3062) to an RH of ~20% (TSI, 2003). Single particles were deposited by diffusion onto TEM grids, a technique described in detail by Freney et al. (2009).

2.3 TEM analysis

Aerosol samples were analyzed with a 200 kV Philips CM200 TEM. The distribution of aerosol particles on TEM grids was not uniform. Coarser particles were deposited near the center of the grid and finer particles on the periphery. Therefore, to ensure that the analyzed particles were representative of the entire size range, three to four areas were chosen from the center and periphery of the sampling spot on each grid. An ellipse was used to fit a particle outline, and the arithmetic mean of the short and long axes of the ellipse was used to determine the particle diameter. In this work, particle detection was accomplished by the method of Li and Shao (2009b, 2010a). Because the particles examined by TEM were dry at the time of observation, this study did not consider the effects of water, other semi-volatile organic aerosols, or NH_4NO_3.

Elemental compositions were semi-quantitatively determined by an energy dispersive X-ray spectrometer (EDS) that can detect elements heavier than C. For some particles, EDS data were combined with selected-area electron diffraction (SAED) to verify their identities. Copper was not considered because of interferences from the copper TEM grid. To understand the internally mixed aerosol particles and their sources, the

ACPD
10, 10589–10623, 2010

composition of different parts of targeted aerosol particles were analyzed in detail (e.g., coatings, inclusions, and coagulations). EDS spectra were collected for 30 s in order to minimize radiation exposure and potential damage.

In earlier work TEM observations of the major aerosol types collected in brown hazes from 30 May to 10 June, 2007, revealed mineral, soot, organic, K-rich, S-rich, fly ash, and metal particles (Li and Shao, 2009a). In this study, we characterize in detail the major aerosol types from ABB, including K-rich, S-rich, soot, and organic particles.

3 Results

3.1 General description of regional haze in northern China

Using Moderate Resolution Imaging Spectroradiometer (MODIS) data, Giovanni has provided high spatial-temporal variability of aerosols on a global scale (Acker and Leptoukh, 2007). Giovanni's AOD map suggests that severe aerosol pollution occurred in northern China (Fig. 1a), with a maximum monthly average AOD at 550 nm of 0.7 in June 2007 (Fig. 1b). Such a high value indicates high PM loading in the troposphere and is related to severe pollution episodes, such as regional brown hazes or Asian dust storms (Du et al., 2008; Eck et al., 1999). Asian dust storms usually begin in late February and end in mid-May (Shao et al., 2008). Therefore, the regional pollution episodes in June are more likely to be the classic brown hazes, in agreement with our observations at the sampling site. The aerosols in the regional hazes were largely contributed by anthropogenic sources, such as industrial emissions, vehicular fossil fuel combustion, and agricultural biomass burning (Li and Shao, 2009a). The hazy days had visibility less than 5 km and wind speeds less than 3 m s^{-1} coming from south of Beijing (Table 1). The regional hazes disappeared in half a day or less and were followed by abrupt cold fronts from the west, only to form again within one day or less during the sampling period. These observations agree with daily mass concentrations of PM_{10} in Beijing. Figure 2 shows that the daily mass concentrations of

ACPD
10, 10589–10623, 2010

PM_{10} and SO_2 in June displayed dramatic changes. The frequent alternation between clear and hazy days is conspicuously noticeable in the sawtooth cycle named by Jia et al. (2008). Eleven samples collected in the five haze episodes (HE-1, HE-2, HE-3, HE-4, and HE-5) were selected for aerosol analysis (Fig. 2). Mass concentrations of PM_{10}, SO_2, and NO_2 on hazy days ranged from 192 to 286 $\mu g\,m^{-3}$, 16 to 48 $\mu g\,m^{-3}$, and 50 to 83 $\mu g\,m^{-3}$, respectively (provided by Beijing Meteorological Bureau). Pollutants on hazy days (peaks in sawtooth cycle) commonly showed a mass concentration 2–3 times higher than pollutants on clear days (valleys in sawtooth cycle), suggesting that the stable meteorological conditions on hazy days favored the accumulation of air pollutants which were slowly transported into adjacent areas.

3.2 The major fine aerosols and their size distribution

3.2.1 Size distribution

The samples collected from brown haze episodes over northern China consisted mainly of mineral, soot, organic compounds, K-rich, S-rich, fly ash, and metal particles (Li and Shao, 2009a). Sizes of the 1066 haze particles, collected during 12–27 June, 2007, ranged from 0.01 to 13 µm with a median diameter of 1.4 µm (Fig. 3). Most of the aerosol particles from anthropogenic sources were in the submicrometer range. Sizes of 470 K- and S-rich particles ranged from 0.01 to 10 µm, with a median diameter of 0.7 µm.

3.2.2 K-rich particles

K-rich particles, one of the abundant inorganic aerosol constituents in brown hazes, are regarded as a tracer of biomass burning and biofuel emissions (Adachi and Buseck, 2008; Engling et al., 2009). Most K-rich particles were irregularly shaped (Fig. 4). EDS measurements showed that they were composed mostly of N, Na, O, S, and K (Fig. 4). Furthermore, diffraction patterns of K-rich particles indicated the presence

ACPD
10, 10589–10623, 2010

of K_2SO_4 and KNO_3. Interestingly, TEM observations showed that K_2SO_4 particles were internally mixed with KNO_3 particles (Fig. 4). The KNO_3 particles were more beam-sensitive than the K_2SO_4 particles, making good diffraction patterns of KNO_3 particles difficult to obtain in this study. These EDS and SAED results are consistent with our observations of the laboratory-generated K_2SO_4 and KNO_3 particles. KCl particles were barely detected in the samples, even though they have been found to be internally mixed with K_2SO_4 and KNO_3 in fresh biomass burning plumes (Li et al., 2003).

3.2.3 S-rich particles

S-rich particles, another of the abundant inorganic aerosol constituents in brown hazes, appeared as subround shapes on TEM grids with their principal elements being N, O, S and minor Na and K (Fig. 5). Although the S-rich particles could have been either ammonium sulfate or ammonium bisulfate, most of their diffraction patterns from SAED matched the structure of crystal ammonium sulfate ($(NH_4)_2SO_4$). In addition, sulfate particles with one or multiple rings of smaller particles (Fig. 5) suggested that these particles were somewhat more acidic than pure ammonium sulfate (Buseck and Posfai, 1999; Sheridan et al., 1993). The abundant $(NH_4)_2SO_4$ particles in Beijing air have been reported to form through chemical reactions between NH_3 and H_2SO_4 (Yao et al., 2003). We also observed that S-rich particles frequently contained minor potassium (Fig. 5), although this result has not been reported previously for Beijing aerosols.

3.2.4 Soot particles

Soot is a combustion product of biofuel, biomass burning, and fossil fuel (Ramanathan and Carmichael, 2008). Soot particles are abundant in urban air and tend to occur as inclusions in K-rich and S-rich particles (Adachi and Buseck, 2008; Li and Shao, 2009a). Soot particles displayed their usual unique morphologies of chains and agglomerates, containing both C and minor O (Fig. 6a). High resolution TEM images

ACPD
10, 10589–10623, 2010

showed that one soot aggregate contained as few as ten to as many as hundreds of carbon spheres with typical diameters from 10 to 50 nm and with some as large as 100 nm. The soot spheres displayed onion-like structures of disordered graphitic layers (Fig. 6b).

3.2.5 Organic aerosols

Li and Shao (2010b) demonstrated that most inorganic particles in brown hazes contained organic coatings and organic inclusions/aggregations. Although the organic inclusion in Fig. 6c can be positively identified in high-magnification images, the organic coatings cannot be. Because of this limitation, we focused on the visible organic aerosols (e.g., organic particle, organic inclusion/aggregation in internally mixed particle) in TEM images.

Most of the organic particles observed in the hazes were internally mixed with K-rich, S-rich, and soot particles, although a few tar balls were observed by Li and Shao (2009a). They contained C and minor amounts of N, O, S, and K. These organic particles were stable under strong electron beam exposures and did not show a graphitic, soot-like structure in high resolution TEM images. Consequently, soot and organic particles were distinguished by their different morphologies.

3.3 Identification of the regional hazes affected by agricultural biomass burning

On the basis of the EDS data for 470 K- and S-rich particles, Fig. 7a further shows that 65% of aerosol particles in HE-1 to HE-3 fell to the left of the K_2SO_4 line, while only 9% in HE-4 to HE-5 did. This difference prompted us to consider these two groups separately, with HE-1 to 3 from 12 to 20 June, 2007 designated as "type-1 haze" and HE-4 to 5 from 21 to 30 June, 2007 designated as "type-2 haze". In Fig. 7a the particles left of the K_2SO_4 line are enriched K with minor S. Based on the EDS measurements and SAED analysis, the major particles on the left are K_2SO_4, KNO_3, or mixtures of both (Figs. 4 and 7b). Excess potassium attributable to fine aerosol particles in air

ACPD
10, 10589–10623, 2010

is a good indicator of biofuel and biomass burning (Reid et al., 1998; Engling et al., 2009). Figure 8a shows that ABB over northern China occurred mainly during 10–20 June, 2007. Prevailing southerly or southeasterly winds in June (Table 1) probably transported these ABB emissions into the regional haze of Beijing. Therefore, the high abundance of K-rich particles in the hazes shown in Fig. 7a, b suggests that intense ABB emissions contributed to type-1 haze rather than type-2 haze. ABB contributed more significantly to the complexity of the K-rich (or S-rich) particles shown in Fig. 7b than to the S-rich particles shown in Fig. 7c. On the other hand, mean values of AOD and water vapor content (WVC) during 12–20 June, 2007, were 2.0 and 2.2, respectively (Fig. 9). Such high values indicate that high numbers of aerosol particles and high WVC occurred in air masses over Beijing (Eck et al., 2005; Fan et al., 2006). In addition, the mean values of AOD and WVC during 21–28 June, 2007, were 1.1 and 2.7, respectively (Fig. 9).

4 Discussion

4.1 Effects of ABB emissions on the brown hazes

Transported ABB emissions not only enhanced atmospheric load but also changed chemical and physical properties of aerosol particles in downwind areas. Li and Shao (2009a) showed that brown hazes over northern China were normally produced by emissions from industry, fossil fuels (e.g., from vehicles and cooking), and soil dust from natural and anthropogenic activities. We assumed that these sources had a constant emission rate throughout the period of the study. During the sampling period, average mass concentrations of daily PM_{10} and SO_2 between the period of 12–20 June to 21–30 June decreased from 192 $\mu g\,m^{-3}$ to 143 $\mu g\,m^{-3}$, and from 37 $\mu g\,m^{-3}$ to 18 $\mu g\,m^{-3}$, respectively (Fig. 2). As the wildfire maps in Fig. 8 show, it can be inferred that the ABB emissions in type-1 haze increased the loadings of PM_{10} and SO_2 in Beijing air. Regional ABB can indeed emit large quantities of fine

ACPD
10, 10589–10623, 2010

primary particles (e.g., organic and K-rich particles), soot, and gases (e.g., VOCs, CO, NO_x, SO_2, and NH_3) into the troposphere (Crutzen and Andreae, 1990). Reid et al. (1998) estimated that condensation and gas-to-particle conversions of inorganic and organic vapors from biomass burning increased the aerosol mass by 20–40%. In addition, the mean WVC value is slightly higher in type-2 haze than in type-1 haze (Fig. 9). This result is consistent with the RH measurements shown in Fig. S1 of the supplementary material, see http://www.atmos-chem-phys-discuss.net/10/10589/2010/acpd-10-10589-2010-supplement.pdf. Bian et al. (2009) indicate that increasing RH can significantly increase the AOD. If we only considered the effect of RH on the AOD, a higher AOD was expected to occur in the type-2 haze than in type-1 haze. In contrast, type 1 haze has a mean AOD twice that of the type 2 haze in this study (see Fig. 9). The most logical explanation was that the intense ABB emissions in the type-1 haze increased the AOD.

Internally mixed fine particles were commonly observed in type-1 haze (Fig. 7b). The high-magnification images in Fig. 10 clearly show that soot and organic particles occurred as inclusions of K- and S-rich particles, and that only small quantities of externally mixed organic and soot particles were observed in the hazes. The result is consistent with our previous investigation of aerosol particles in the brown hazes from 31 May to 11 June (Li and Shao, 2009a). The internal mixtures mean that soot particles underwent aging processes of condensation and coagulation. The aged soot particles shown in Fig. 10e–g eventually became hydrophilic when they were coated with water-soluble compounds such as $(NH_4)_2SO_4$, NH_4HSO_4, KNO_3, K_2SO_4, or oxidized organic particles, implying that soot particles were important nuclei for the development of fine particles in the hazes.

Abundant KCl particles have been detected in fresh smoke plumes of biomass burning, and they are transformed through heterogeneous chemical reactions to K_2SO_4 and KNO_3 (Engling et al., 2009; Li et al., 2003; Posfai et al., 2003). The dominant K_2SO_4 and KNO_3 particles and absence of KCl particles in type-1 haze suggested that KCl particles from ABB experienced heterogeneous reactions with nitric acid and sulfuric

ACPD
10, 10589–10623, 2010

acid in the atmosphere, prior to the sampling site. In addition, the S-rich particles in type-1 haze often contained minor K, but the minor K-salts could not be identified by their morphologies (Fig. 5). A similar mixture was also observed in smoke-hazes in Mexico (Yokelson et al., 2009).

4.2 Understanding the mixing mechanisms of ambient aerosol particles

Knowing the mixing mechanisms would be instructive for understanding the formation of the regional hazes and would shed light on heterogeneous reaction mechanisms which cannot be determined by bulk methods. When we consider the TEM results of aerosol particles as well as their ambient environments, the mixing processes of the internally mixed particles can be reasonably explained.

Aerosol particles in the atmosphere usually exhibit different properties due to different ambient environments (e.g., humidity) (Martin, 2000; Semeniuk et al., 2007; Wise et al., 2005). Martin (2000) indicates that comprehensive laboratory work in the atmospheric sciences has provided the phase transitions of deliquescence and efflorescence of many salts with changes in RH. Solid particles of $(NH_4)_2SO_4$, KNO_3, and K_2SO_4 can deliquesce into aqueous particles at RH of 79%, 93%, and 96%, respectively (Table S1, http://www.atmos-chem-phys-discuss.net/10/10589/2010/acpd-10-10589-2010-supplement.pdf) (Cziczo et al., 1997; Freney et al., 2009). Internally mixed salt particles generally have a mutual deliquescence RH that is lower than either of the pure salts (Freney et al., 2009). As shown in Fig. S1, KNO_3, K_2SO_4, and $(NH_4)_2SO_4$ particles became aqueous because of the elevated early-morning RHs close to 96%. Once these particles deliquesce, the aqueous droplets easily capture the refractory soot and organic particles. This argument is also supported by our observations that K- and S-rich particles with refractory inclusions of soot and organics (Fig. 10) frequently occurred in the samples.

The water-dialysis of individual particles conducted by Li and Shao (2010b) showed that the organic compounds coated on K- and S-rich particles in brown hazes over Beijing were mostly soluble. The hydrophobic organic particles from biomass burn-

ACPD
10, 10589–10623, 2010

ing, which coagulate and condense on inorganic particles, can be oxidized and act as hygroscopic coatings during transport (Rudich et al., 2007; Semeniuk et al., 2007; Li and Shao, 2010b). The hygroscopic organic coatings may enhance water uptake of inorganic particles at lower humidity (Brooks et al., 2002; Mikhailov et al., 2009), and decrease the efflorescence RH of inorganic particles significantly (Parsons et al., 2004). Additionally, acidic particles (Figs. 5 and 10e) are more hygroscopic than pure $(NH_4)_2SO_4$ and so contain more water. The aging of ABB particles can enhance the hygroscopicity of the fine particles, likely increasing the mixing rate among aerosol particles in Beijing air. Once deliquescence of the mixtures of organic and inorganic particles shown in Fig. 10a–d occurs, the aqueous particles attain larger particle sizes and scatter solar radiation more efficiently than solid particles (Martin et al., 2004). Furthermore, internally mixed soot, shown in Fig. 10e–g, is more absorbent than externally mixed soot (Jacobson, 2001).

4.3 Further considerations about regional brown hazes over China

Field observations show that the brown hazes displayed some similar characteristics, such as gray sky, low visibility, and a high load of PM, but aerosol particles in different hazes exhibited different elemental compositions, morphologies, and mixing states. Furthermore, differences in the chemical and physical properties of fine aerosol particles in different haze types (e.g., dust-haze, smoke brown haze, and non-smoke brown haze) also impacted the regional and global climates differently (Wang et al., 2009). Therefore, we not only need to identify the haze types, but we also need to consider properties of individual aerosol particles in different hazes. In particular, emissions from ABB in large and widespread areas produce high concentrations of gases and fine particles for brief periods each year. These gases and fine particles enhance both the formation of secondary particles and acids (H_2SO_4, HNO_3, and various organic acids) and their coagulation and condensation onto inorganic particles, resulting in significant changes to their physical and chemical properties (Bein et al., 2008). More importantly, however, high WVC during brown hazes can promote the hygroscopic

ACPD
10, 10589–10623, 2010

growth of K-rich, S-rich, and organic particles, or their mixtures. The positive correlation ($R = 0.9$) between AOD and WVC during the type-1 haze shown in Fig. 9 further suggests that particle counts are extremely high and that they are growing hygroscopically (Li et al., 2007). Whenever RH is elevated, its importance on AOD is substantially amplified because the aerosols are hygroscopic (Bian et al., 2009). In addition, the AOD of aged soot in polluted air is considerably increased over that of fresh soot and correlates strongly with RH (Zhang et al., 2008), leading to even greater decreases in visibility.

Morning and nighttime humidity in June normally reaches 80% or higher but then decreases to between 20 and 60% from midday to late afternoon (see Fig. S1). Therefore, when we consider the climate effects of aerosol particles in regional haze, solid and aqueous states of the hygroscopic particles should be evaluated at different humidities. The variation of humidity during a haze episode can create a multi-cycle transformation of the soluble particles between an aqueous and solid phase. Once these aged particles in haze trap water vapor on their surfaces, their hydrological cycle changes as they are transported on a regional scale.

The high AOD values over northern China suggest that the haze aerosols reduce solar flux on the ground and cool the surface atmosphere (Li et al., 2007). In contrast, the internally mixed soot particles in regional hazes probably absorb solar radiation and heat the upper atmosphere over northern China. Recent observations of radiative forcing from aerosols in regional hazes over northern China show that aerosol particles under hazy weather conditions generate a positive heating effect on the atmospheric column (Wang et al., 2009; Xia et al., 2006). Once aerosols alter the radiation budgets of the lower and upper atmospheres, a haze episode may persist because the atmosphere becomes more stable. Furthermore, the variation may affect the development and microphysics of clouds by reducing vertical heat exchange and restricting convective transport (Fan et al., 2008). Significantly, these aged fine aerosol particles shown in Fig. 10 can be transported great distances and have the ability to carry air toxics such as heavy metals and PAHs (Guilloteau et al., 2009; Li and Shao, 2009a). The

ACPD
10, 10589–10623, 2010

adverse effects of these aerosol particles on human health merit serious attention.

5 Conclusions

Giovanni's aerosol optical depth (AOD) map shows that the monthly average AOD at 550 nm in the region had its maximum value (0.7) in June 2007. Such a high AOD value suggests that some unique brown haze episodes occurred during this time period. The morphology, composition, and mixing state of individual aerosol particles were characterized using TEM/EDS. Abundant potassium salts (K_2SO_4 and KNO_3) were present in fine particles collected during 12–20 June but were absent during 21–30 June, 2007. This difference prompted us to separate the haze episodes into two categories, with HE-1 to HE-3 (12–20 June) being termed as "type-1 haze", and HE-4 to HE-5 (21–30 June) being termed as "type-2 haze". The abundant potassium-dominant particles indicated that biomass burning emissions contributed heavily to type-1 haze. MODIS wildfire maps showed that intensive ABB in northern China occurred frequently from 10 to 20 June, 2007. We conclude, therefore, that in just a few days ABB emissions after long-range transport can significantly influence air quality in Beijing.

The copious organic particles, soot particles, and gases emitted by ABB enhance the formation of secondary particles and the coagulation of pre-existing inorganic particles, resulting in more complex aerosol particles in type-1 haze than in type-2 haze. Soot particles were generally mixed with potassium salts, ammonium salts, and organic particles. The aging process of aerosol particles from ABB altered their optical properties. In particular, the soot particles internally mixed with sulfates increases the absorption of visible solar radiation when compared to soot alone (Jacobson, 2001). In addition, abundant K_2SO_4 and KNO_3 particles in the absence of KCl illustrate that aerosol particles emitted by ABB underwent an extensive aging process during their transport to the sampling site. Therefore, ABB emissions after long-range transport not only increased the atmospheric loadings of urban pollutants but also changed the chemical and physical properties of aerosol particles in downwind areas. Furthermore,

ACPD
10, 10589–10623, 2010

we concluded that the ABB contribution increased AOD in type-1 haze twice as much as the AOD in type-2 haze.

Understanding the mixing states and elemental compositions of ABB particles in the regional hazes will allow a better estimate of the hygroscopic growth of these particles under ambient RH conditions. Therefore, when considering the regional climate of the haze episodes over northern China, we need to consider the contribution from ABB. In addition to their impacts on climate change, the elevated concentrations of fine particles in Beijing air, a substantial portion of which comes from ABB, adversely affects human health. As the most populous and fastest developing country in the world, China must recognize the heavy aerosol loadings in regional haze episodes and take steps to reduce their concentrations to enhance the respiratory health of its citizens.

Acknowledgements. We thank Wei Wang for assistance with sample collection and Evelyn Freney for providing laboratory-generated K_2SO_4/KNO_3 sample. We appreciate Kouji Adachi's comments. We appreciate Peter Buseck for his sponsoring the visit of WJL to Arizona State University. We acknowledge the use of the TEMs in the LeRoy Eyring Center for Solid State Science at Arizona State University. Analyses and visualizations used in this study were produced with the Giovanni online data system, developed and maintained by the NASA Goddard Earth Sciences (GES) Data and Information Services Center (DISC). Financial support was provided by National Basic Research Program of China (2006CB403701), State Key Laboratory of Coal Resources and Safe Mining (SKLCRSM09KFB04), China Postdoctoral Science Foundation funded project (20090461213), and Shandong Postdoctoral Science Innovation Foundation (200902016).

References

Acker, G. and Leptoukh, G.: Online Analysis Enhances Use of NASA Earth Science Data, Eos, Trans. AGU, 88(2), 14–17, 2007.

Adachi, K. and Buseck, P. R.: Internally mixed soot, sulfates, and organic matter in aerosol particles from Mexico City, Atmos. Chem. Phys., 8, 6469–6481, 2008, http://www.atmos-chem-phys.net/8/6469/2008/.

Andreae, M. O., Rosenfeld, D., Artaxo, P., Costa, A. A., Frank, G. P., Longo, K. M., and Silva-Dias, M. A. F.: Smoking Rain Clouds over the Amazon, Science, 303(5662), 1337–1342, 2004.

Bein, K. J., Zhao, Y. J., Johnston, M. V., and Wexler, A. S.: Interactions between boreal wildfire and urban emissions, J. Geophys. Res., 113(D7), D07304, doi:10.1029/2007JD008910, 2008.

Bian, H., Chin, M., Rodriguez, J. M., Yu, H., Penner, J. E., and Strahan, S.: Sensitivity of aerosol optical thickness and aerosol direct radiative effect to relative humidity, Atmos. Chem. Phys., 9, 2375–2386, 2009, http://www.atmos-chem-phys.net/9/2375/2009/.

Bowman, D. M. J. S., Balch, J. K., Artaxo, P., Bond, W. J., Carlson, J. M., Cochrane, M. A., D'Antonio, C. M., DeFries, R. S., Doyle, J. C., Harrison, S. P., Johnston, F. H., Keeley, J. E., Krawchuk, M. A., Kull, C. A., Marston, J. B., Moritz, M. A., Prentice, I. C., Roos, C. I., Scott, A. C., Swetnam, T. W., van der Werf, G. R., and Pyne, S. J.: Fire in the Earth System, Science, 324(5926), 481–484, 2009.

Brooks, S. D., Wise, M. E., Cushing, M., and Tolbert, M. A.: Deliquescence behavior of organic/ammonium sulfate aerosol, Geophys. Res. Lett., 29(19), 1917, doi:10.1029/2002GL014733, 2002.

Buseck, P. R. and Posfai, M.: Airborne minerals and related aerosol particles: Effects on climate and the environment, P. Natl. Acad. Sci. USA, 96(7), 3372–3379, 1999.

Cao, G. L., Zhang, X. Y., Wang, Y. Q., and Zheng, F. C.: Estimation of emissions from field burning of crop straw in China, Chin. Sci. Bull., 53(5), 784–790, 2008.

Chung, S. H. and Seinfeld, J. H.: Global distribution and climate forcing of carbonaceous aerosols, J. Geophys. Res., 107(D19), doi:10.1029/2001JD001397, 4407, 2002.

Crutzen, P. J. and Andreae, M. O.: Biomass burning in the tropics-impact on atmospheric chemistry and biogeochemical cycles, Science, 250(4988), 1669–1678, 1990.

Cziczo, D. J., Nowak, J. B., Hu, J. H., and Abbatt, J. P. D.: Infrared spectroscopy of model tropospheric aerosols as a function of relative humidity: Observation of deliquescence and crystallization, J. Geophys. Res., 102(D15), 18843–18850, 1997.

Da Rocha, G. O., Allen, A. G., and Cardoso, A. A.: Influence of agricultural biomass burning on aerosol size distribution and dry deposition in southeastern Brazil, Environ. Sci. Technol., 39(14), 5293–5301, 2005.

de Gouw, J. A., Cooper, O. R., Warneke, C., Hudson, P. K., Fehsenfeld, F. C., Holloway, J. S.,

Hubler, G., Nicks, D. K., Nowak, J. B., Parrish, D. D., Ryerson, T. B., Atlas, E. L., Donnelly, S. G., Schauffler, S. M., Stroud, V., Johnson, K., Carmichael, G. R., and Streets, D. G.: Chemical composition of air masses transported from Asia to the U. S. West Coast during ITCT 2K2: Fossil fuel combustion versus biomass-burning signatures, J. Geophys. Res.-Atmos., 109(D23), D23S20, doi:10.1029/2003JD004202, 2004.

Du, W. P., Xin, J. Y., Wang, M. X., Gao, Q. X., Li, Z. Q., and Wang, Y. S.: Photometric measurements of spring aerosol optical properties in dust and non-dust periods in China, Atmos. Environ., 42(34), 7981–7987, 2008.

Duan, F. K., Liu, X. D., Yu, T., and Cachier, H.: Identification and estimate of biomass burning contribution to the urban aerosol organic carbon concentrations in Beijing, Atmos. Environ., 38(9), 1275–1282, 2004.

Eck, T. F., Holben, B. N., Reid, J. S., Dubovik, O., Smirnov, A., O'Neill, N. T., Slutsker, I., and Kinne, S.: Wavelength dependence of the optical depth of biomass burning, urban, and desert dust aerosols, J. Geophys. Res., 104(D24), 31333–31349, 1999.

Eck, T. F., Holben, B. N., Dubovik, O., Smirnov, A., Goloub, P., Chen, H. B., Chatenet, B., Gomes, L., Zhang, X. Y., Tsay, S. C., Ji, Q., Giles, D., and Slutsker, I.: Columnar aerosol optical properties at AERONET sites in central eastern Asia and aerosol transport to the tropical mid-Pacific, J. Geophys. Res., 110(D6), D06202, doi:10.1029/2004JD005274, 2005.

Engling, G., Lee, J. J., Tsai, Y.-W., Lung, S.-C. C., Chou, C. C. K., and Chan, C.-Y.: Size-Resolved Anhydrosugar Composition in Smoke Aerosol from Controlled Field Burning of Rice Straw, Aerosol. Sci. Tech., 43(7), 662–672, 2009.

Fan, J., Zhang, R., Tao, W.-K., and Mohr, K. I.: Effects of aerosol optical properties on deep convective clouds and radiative forcing, J. Geophys. Res., 113, D08209, doi:10.1029/2007JD009257, 2008.

Fan, X., Chen, H., Goloub, P., Xia, X. A., Zhang, W., and Chatenet, B.: Analysis of column-integrated aerosol optical thickness in beijing from aeronet observations, China Particuology, 4(6), 330–335, 2006.

Freney, E. J., Martin, S. T., and Buseck, P. R.: Deliquescence and Efflorescence of Potassium Salts Relevant to Biomass-Burning Aerosol Particles, Aerosol. Sci. Tech., 43(8), 799–807, 2009.

Fuller, K. A., Malm, W. C., and Kreidenweis, S. M.: Effects of mixing on extinction by carbonaceous particles, J. Geophys. Res., 104, 15941–15954, 1999.

Guilloteau, A., Bedjanian, Y., Nguyen, M. L., and Tomas, A.: Desorption of Polycyclic Aromatic

Hydrocarbons from a Soot Surface: Three- to Five-Ring PAHs, J. Phys. Chem. A, 114(2), 942–948, 2009.

IPCC: Climate Change 2007: The Physical Science Basis, Contribution of Working Group I to the Fourth Assessment Report of the Intergovernmental Panel on Climate Change, edited by: Solomon, S., Qin, D., Manning, M., Chen, Z., Marquis, M., Averyt, K. B., Tignor, M., and Miller, H. L., Cambridge University Press, Cambridge, United Kingdom and New York, NY, USA, 2007.

Jacob, D. J., Crawford, J. H., Kleb, M. M., Connors, V. S., Bendura, R. J., Raper, J. L., Sachse, G. W., Gille, J. C., Emmons, L., and Heald, C. L.: Transport and Chemical Evolution over the Pacific (TRACE-P) aircraft mission: Design, execution, and first results, J. Geophys. Res., 108(D20), 9000, doi:10.1029/2002JD003276, 2003.

Jacobson, M. Z.: Strong radiative heating due to the mixing state of black carbon in atmospheric aerosols, Nature, 409(6821), 695–697, 2001.

Jaffe, D., Anderson, T., Covert, D., Kotchenruther, R., Trost, B., Danielson, J., Simpson, W., Berntsen, T., Karlsdottir, S., Blake, D., Harris, J., Carmichael, G., and Uno, I.: Transport of Asian air pollution to North America, Geophys. Res. Lett., 26(6), 711–714, 1999.

Jia, Y. T., Rahn, K. A., He, K. B., Wen, T. X., and Wang, Y. S.: A novel technique for quantifying the regional component of urban aerosol solely from its sawtooth cycles, J. Geophys. Res., 113(D21), D21309, doi:10.1029/2008JD010389, 2008.

Johnson, K. S., Zuberi, B., Molina, L. T., Molina, M. J., Iedema, M. J., Cowin, J. P., Gaspar, D. J., Wang, C., and Laskin, A.: Processing of soot in an urban environment: case study from the Mexico City Metropolitan Area, Atmos. Chem. Phys., 5, 3033–3043, 2005, http://www.atmos-chem-phys.net/5/3033/2005/.

Koe, L. C. C., Arellano, A. F., and McGregor, J. L.: Investigating the haze transport from 1997 biomass burning in Southeast Asia: its impact upon Singapore, Atmos. Environ., 35(15), 2723–2734, 2001.

Lesins, G., Chylek, P., and Lohmann, U.: A study of internal and external mixing scenarios and its effect on aerosol optical properties and direct radiative forcing, J. Geophys. Res., 107(D10), 4049, doi:10.1029/2001JD000973, 2002.

Li, J., Posfai, M., Hobbs, P. V., and Buseck, P. R.: Individual aerosol particles from biomass burning in southern Africa: 2, Compositions and aging of inorganic particles, J. Geophys. Res., 108(D13), 8484, doi:10.1029/2002JD002310, 2003.

Li, W. J. and Shao, L. Y.: Transmission electron microscopy study of aerosol par-

ticles from the brown hazes in northern China, J. Geophys. Res., 114, D09302, doi:10.1029/2008JD011285, 2009a.
Li, W. J. and Shao, L. Y.: Observation of nitrate coatings on atmospheric mineral dust particles, Atmos. Chem. Phys., 9, 1863–1871, 2009, http://www.atmos-chem-phys.net/9/1863/2009/.
Li, W. J. and Shao, L. Y.: Characterization of mineral particles in winter fog of Beijing analyzed by TEM and SEM, Environ. Monit. Assess., 161(1), 565–573, 2010a.
Li, W. J. and Shao, L. Y.: Mixing and water-soluble characteristics of particulate organic compounds in individual urban aerosol particles, J. Geophys. Res., 115, D02301, doi:10.1029/2009JD012575, 2010b.
Li, Z. Q., Xia, X. G., Cribb, M., Mi, W., Holben, B., Wang, P. C., Chen, H. B., Tsay, S. C., Eck, T. F., Zhao, F. S., Dutton, E. G., and Dickerson, R. E.: Aerosol optical properties and their radiative effects in northern China, J. Geophys. Res., 112(D22), D22S01, doi:10.1029/2006JD007382, 2007.
Ma, Y., Weber, R. J., Lee, Y. N., Orsini, D. A., Maxwell-Meier, K., Thornton, D. C., Bandy, A. R., Clarke, A. D., Blake, D. R., Sachse, G. W., Fuelberg, H. E., Kiley, C. M., Woo, J. H., Streets, D. G., and Carmichael, G. R.: Characteristics and influence of biosmoke on the fine-particle ionic composition measured in Asian outflow during the Transport and Chemical Evolution Over the Pacific (TRACE-P) experiment, J. Geophys. Res., 108(D21), 8816, doi:10.1029/2002JD003128, 2003.
Martin, S. T.: Phase transitions of aqueous atmospheric particles, Chem. Rev., 100(9), 3403–3453, 2000.
Martin, S. T., Hung, H.-M., Park, R. J., Jacob, D. J., Spurr, R. J. D., Chance, K. V., and Chin, M.: Effects of the physical state of tropospheric ammonium-sulfate-nitrate particles on global aerosol direct radiative forcing, Atmos. Chem. Phys., 4, 183–214, 2004, http://www.atmos-chem-phys.net/4/183/2004/.
Mikhailov, E., Vlasenko, S., Martin, S. T., Koop, T., and Pöschl, U.: Amorphous and crystalline aerosol particles interacting with water vapor: conceptual framework and experimental evidence for restructuring, phase transitions and kinetic limitations, Atmos. Chem. Phys., 9, 9491–9522, 2009, http://www.atmos-chem-phys.net/9/9491/2009/.
Niemi, J. V., Tervahattu, H., Vehkamäki, H., Martikainen, J., Laakso, L., Kulmala, M., Aarnio, P., Koskentalo, T., Sillanpää, M., and Makkonen, U.: Characterization of aerosol particle

episodes in Finland caused by wildfires in Eastern Europe, Atmos. Chem. Phys., 5, 2299–2310, 2005, http://www.atmos-chem-phys.net/5/2299/2005/.

Parsons, M. T., Knopf, D. A., and Bertram, A. K.: Deliquescence and Crystallization of Ammonium Sulfate Particles Internally Mixed with Water-Soluble Organic Compounds, J. Phys. Chem. A, 108(52), 11600–11608, 2004.

Peltier, R. E., Hecobian, A. H., Weber, R. J., Stohl, A., Atlas, E. L., Riemer, D. D., Blake, D. R., Apel, E., Campos, T., and Karl, T.: Investigating the sources and atmospheric processing of fine particles from Asia and the Northwestern United States measured during INTEX B, Atmos. Chem. Phys., 8, 1835–1853, 2008, http://www.atmos-chem-phys.net/8/1835/2008/.

Posfai, M., Anderson, J. R., Buseck, P. R., and Sievering, H.: Soot and sulfate aerosol particles in the remote marine troposphere, J. Geophys. Res., 104(D17), 21685–21693, 1999.

Posfai, M., Simonics, R., Li, J., Hobbs, P. V., and Buseck, P. R.: Individual aerosol particles from biomass burning in southern Africa: 1. Compositions and size distributions of carbonaceous particles, J. Geophys. Res., 108(D13), 8483, doi:10.1029/2002JD002291, 2003.

Ramanathan, V. and Carmichael, G.: Global and regional climate changes due to black carbon, Nature Geosci., 1(4), 221–227, 2008.

Reid, J. S., Hobbs, P. V., Ferek, R. J., Blake, D. R., Martins, J. V., Dunlap, M. R., and Liousse, C.: Physical, chemical, and optical properties of regional hazes dominated by smoke in Brazil, J. Geophys. Res., 103(D24), 32059–32080, 1998.

Reid, J. S., Koppmann, R., Eck, T. F., and Eleuterio, D. P.: A review of biomass burning emissions part II: intensive physical properties of biomass burning particles, Atmos. Chem. Phys., 5, 799–825, 2005, http://www.atmos-chem-phys.net/5/799/2005/.

Roberts, G. C., Nenes, A., Seinfeld, J. H., and Andreae, M. O.: Impact of biomass burning on cloud properties in the Amazon Basin, J. Geophys. Res., 108(D2), 4062, doi:10.1029/2001JD000985, 2003.

Rudich, Y., Donahue, N. M., and Mentel, T. F.: Aging of organic aerosol: Bridging the gap between laboratory and field studies, Annu. Rev. Phys. Chem., 58, 321–352, 2007.

Semeniuk, T. A., Wise, M. E., Martin, S. T., Russell, L. M., and Buseck, P. R.: Hygroscopic behavior of aerosol particles from biomass fires using environmental transmission electron microscopy, J. Atmos. Chem., 56(3), 259–273, 2007.

Shao, L. Y., Li, W. J., Xiao, Z. H., and Sun, Z. Q.: The mineralogy and possible sources of spring dust particles over Beijing, Adv. Atmos. Sci., 25(3), 395–403, 2008.
Sheridan, P. J., Schnell, R. C., Kahl, J. D., Boatman, J. F., and Garvey, D. M.: Microanalysis of the aerosol collected over south-central New Mexico during the alive field experiment, May–December 1989, Atmos. Environ., 27(8), 1169–1183, 1993.
Wang, Y., Che, H., Ma, J., Wang, Q., Shi, G., Chen, H., Goloub, P., and Hao, X.: Aerosol radiative forcing under clear, hazy, foggy, and dusty weather conditions over Beijing, China, Geophys. Res. Lett., 36, L06804, doi:10.1029/2009GL037181, 2009.
Wise, M. E., Biskos, G., Martin, S. T., Russell, L. M., and Buseck, P. R.: Phase transitions of single salt particles studied using a transmission electron microscope with an environmental cell, Aerosol. Sci. Tech., 39(9), 849–856, 2005.
Xia, X. A., Chen, H. B., Wang, P. C., Zhang, W. X., Goloub, P., Chatenet, B., Eck, T. F., and Holben, B. N.: Variation of column-integrated aerosol properties in a Chinese urban region, J. Geophys. Res., 111(D5), D05204, doi:10.1029/2005JD006203, 2006.
Yang, M., Howell, S. G., Zhuang, J., and Huebert, B. J.: Attribution of aerosol light absorption to black carbon, brown carbon, and dust in China interpretations of atmospheric measurements during EAST-AIRE, Atmos. Chem. Phys., 9, 2035–2050, 2009, http://www.atmos-chem-phys.net/9/2035/2009/.
Yao, X., Lau, A. P. S., Fang, M., Chan, C. K., and Hu, M.: Size distributions and formation of ionic species in atmospheric particulate pollutants in Beijing, China: 1-inorganic ions, Atmos. Environ., 37(21), 2991–3000, 2003.
Yienger, J. J., Galanter, M., Holloway, T. A., Phadnis, M. J., Guttikunda, S. K., Carmichael, G. R., Moxim, W. J., and Levy, H.: The episodic nature of air pollution transport from Asia to North America, J. Geophys. Res.-Atmos., 105(D22), 26931–26945, 2000.
Yokelson, R. J., Crounse, J. D., DeCarlo, P. F., Karl, T., Urbanski, S., Atlas, E., Campos, T., Shinozuka, Y., Kapustin, V., Clarke, A. D., Weinheimer, A., Knapp, D. J., Montzka, D. D., Holloway, J., Weibring, P., Flocke, F., Zheng, W., Toohey, D., Wennberg, P. O., Wiedinmyer, C., Mauldin, L., Fried, A., Richter, D., Walega, J., Jimenez, J. L., Adachi, K., Buseck, P. R., Hall, S. R., and Shetter, R.: Emissions from biomass burning in the Yucatan, Atmos. Chem. Phys., 9, 5785–5812, 2009, http://www.atmos-chem-phys.net/9/5785/2009/.
Zhang, R. Y., Khalizov, A. F., Pagels, J., Zhang, D., Xue, H. X., and McMurry, P. H.: Variability in morphology, hygroscopicity, and optical properties of soot aerosols during atmospheric

ACPD
10, 10589–10623, 2010

processing, P. Natl. Acad. Sci. USA, 105(30), 10291–10296, 2008.
Zhang, Y. X., Shao, M., Zhang, Y. H., Zeng, L. M., He, L. Y., Zhu, B., Wei, Y. J., and Zhu, X. L.: Source profiles of particulate organic matters emitted from cereal straw burnings, J. Environ. Sci., 19(2), 167–175, 2007.

Table 1. Information of the analyzed samples collected in urban Beijing.

Date	Start Time	T	RH	RH	P	WS	WD	V
	UTC	°C	%	Max, %	hPa	($m\,s^{-1}$)		km
12/06/2007	09:30	20	62	67	1000	2	SE	3
17/06/2007	09:45	30	42	48	999	3	SSE	4
19/06/2007	02:30	31	44	51	1004	2	WSS	3
19/06/2007	05:30	32	50	53	1002	1	SSE	0.5
20/06/2007	07:00	28	66	69	1001	3	S	2
21/06/2007	03:00	36	36	39	999	2	WS	3
23/06/2007	04:00	28	62	65	993	2	SE	3
23/06/2007	04:10	28	62	65	993	2	SE	3
27/06/2007	02:00	32	64	67	991	3	SEE	2
27/06/2007	02:10	32	64	67	991	3	SEE	2
27/06/2007	05:45	24	70	75	991	8	WSS	4

T – temperature, RH – relative humidity, P – barometric pressure, WS – wind speed, WD – wind direction, V – visibility.

ACPD
10, 10589–10623, 2010

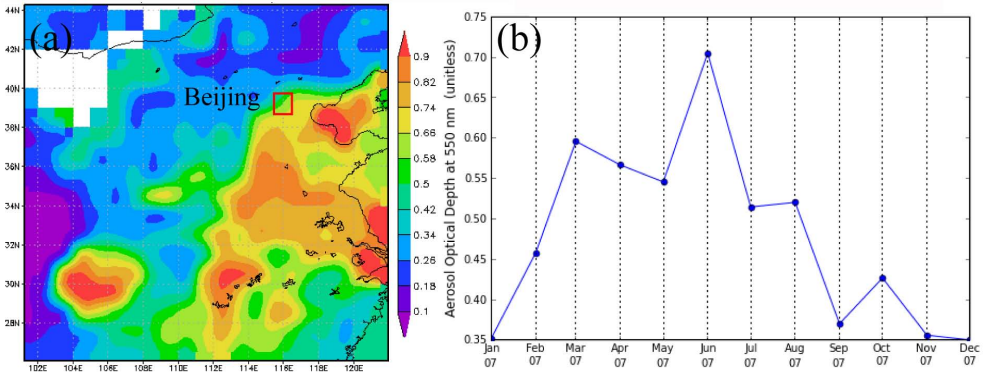

Fig. 1. Aerosol optical depth (AOD) map and monthly average AOD of area-averaged time series over northern China (region: 101.25° E–121.99 E, 26.02° N–44.30° N) derived from MODIS-Terra data from January to December 2007 (http://disc.sci.gsfc.nasa.gov/giovanni/). **(a)** Mean AOD value at 550 nm from January to December 2007. **(b)** Monthly mean AOD value in 2007.

ACPD
10, 10589–10623, 2010

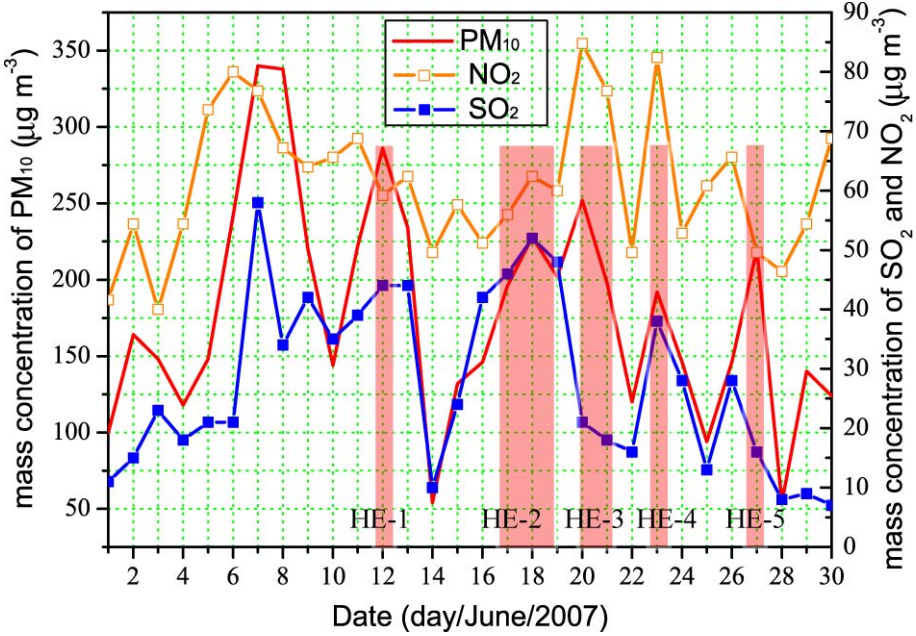

Fig. 2. Daily mass concentrations of PM_{10}, SO_2, and NO_2 in Beijing in June 2007 (http://datacenter.mep.gov.cn/). Sample collection was conducted during the five haze episodes (HE-1, HE-2, HE-3, HE-4, and HE-5), which were marked by the vertical column.

ACPD
10, 10589–10623, 2010

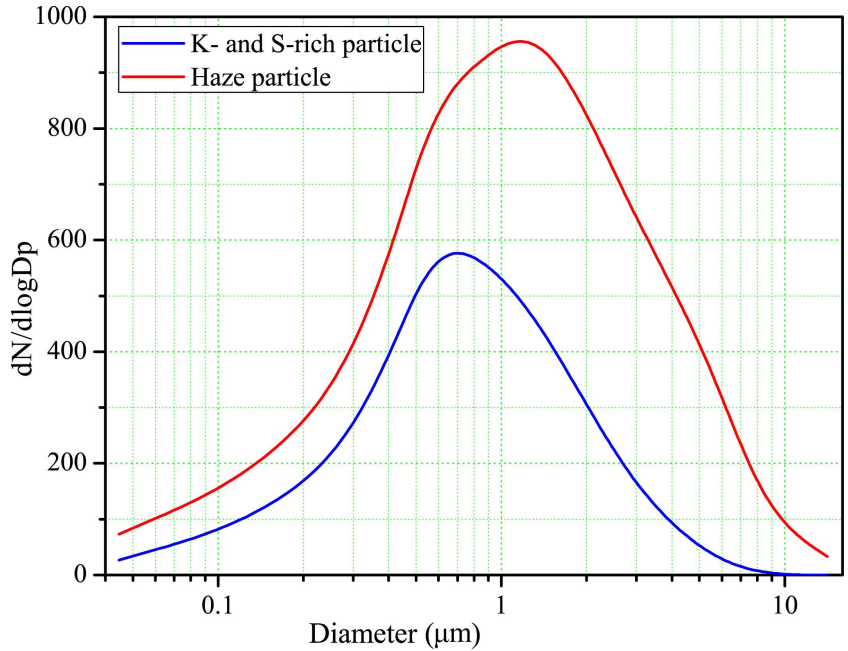

Fig. 3. Size distributions of 1066 haze particles (i.e., mineral, soot, organic, K-rich, S-rich, fly ash, and metal particles) and 470 K- and S-rich particles. The K- and S-rich particles were internally mixed with soot and/or organic particles.

ACPD
10, 10589–10623, 2010

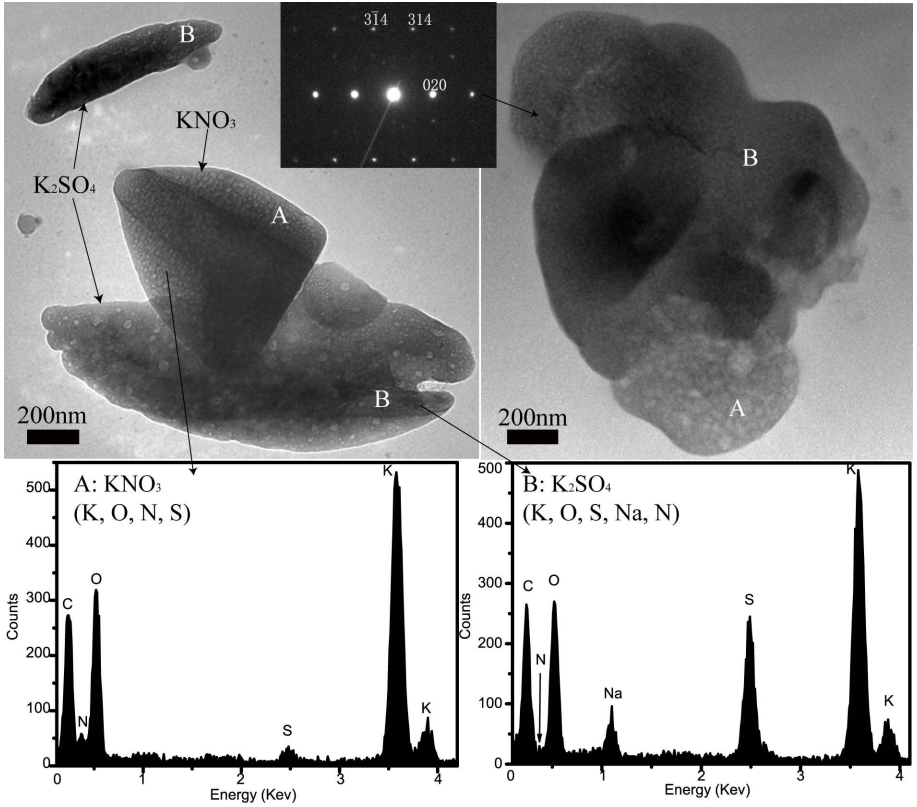

Fig. 4. Mixtures of K_2SO_4 **(B)** and KNO_3 **(A)** particles based on their elemental compositions and crystal structures from EDS and SAED. Diffraction pattern of K_2SO_4 was indexed. The KNO_3 particle is more beam sensitive than the K_2SO_4 particle.

ACPD
10, 10589–10623, 2010

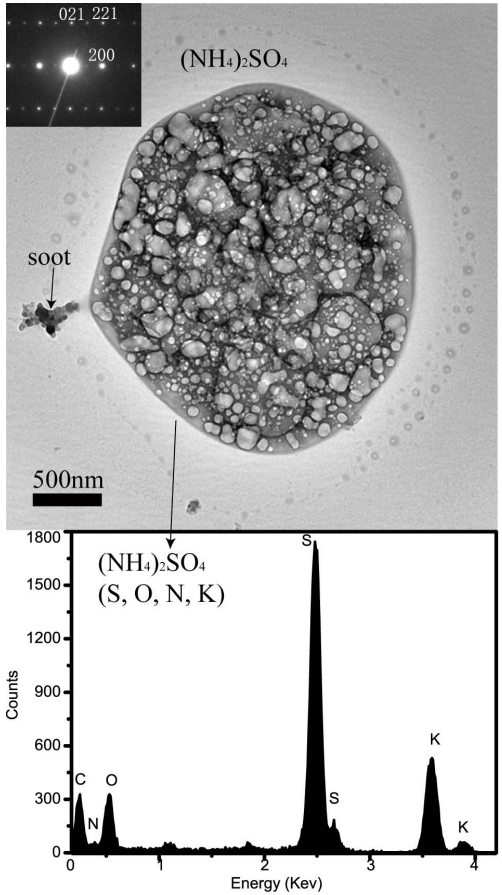

Fig. 5. Elemental compositions of S-rich particles collected during the hazes also contain N, O, and K. Minor K-rich salts could be internally mixed within $(NH_4)_2SO_4$. The diffraction pattern was obtained from another similar-looking particle, which was totally damaged during electron beam exposure.

ACPD
10, 10589–10623, 2010

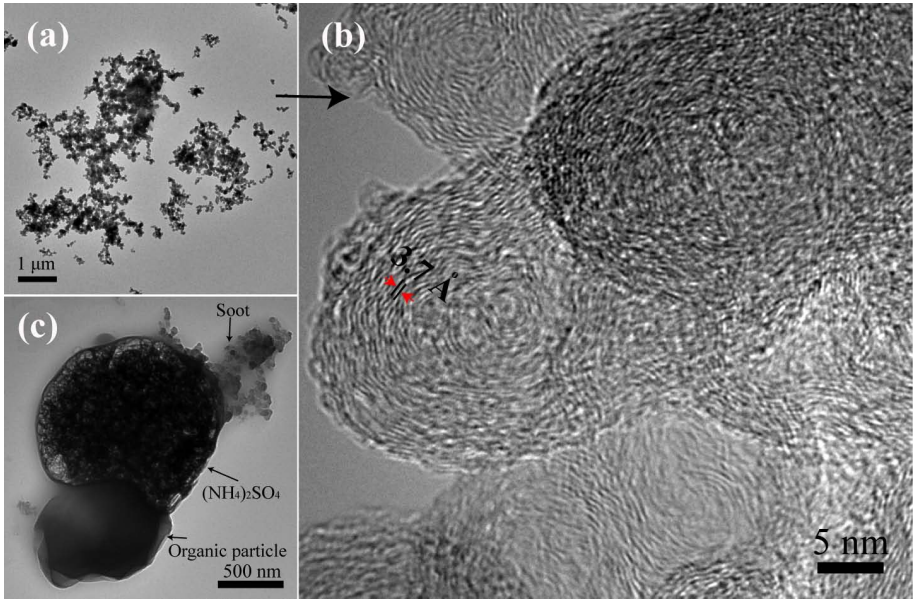

Fig. 6. Transmission electron microscopy images of soot aggregates and organic particle. **(a)** TEM image of chain-like soot aggregate in regional hazes. **(b)** High resolution TEM image of soot. The soot spheres display onion-like structures of disordered graphitic layers. **(c)** Mixture of organic, ammonium sulfate, and soot particle.

ACPD
10, 10589–10623, 2010

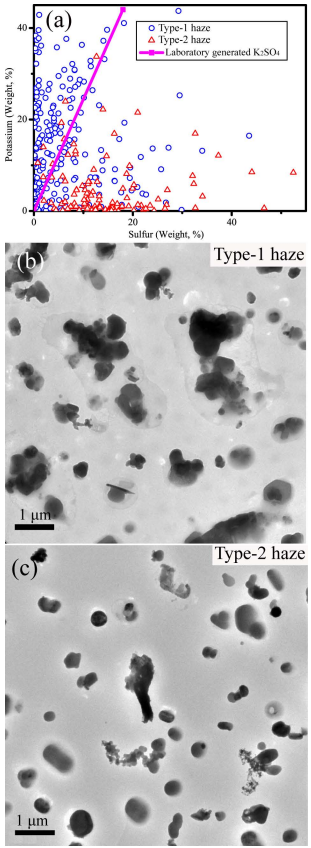

Fig. 7. Comparisons of morphologies and elemental compositions of individual fine particles of different haze episodes. Each open triangle represents weight percentage of S and K in each measured particle. The solid line indicates the average weight percentage of S and K in the K_2SO_4 particles generated in laboratory. **(a)** Separation of type-1 haze (i.e., H1, H2, and H3) during 12–20 June and type-2 haze (i.e., H4 and H5) during 21–30 June according to the potassium content in aerosol particles. **(b)** Morphologies of aerosol particles in type-1 haze. **(c)** Morphologies of aerosol particles in type-2 haze.

ACPD
10, 10589–10623, 2010

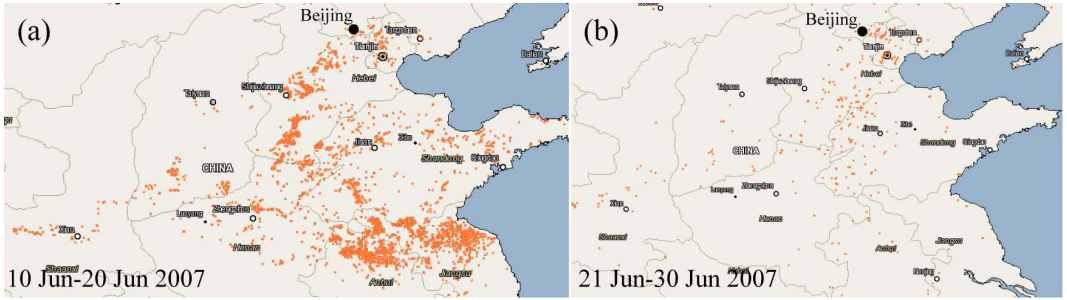

Fig. 8. Two ABB maps over northern China. **(a)** Intensive ABB scattered in northern China located in south of Beijing during 10–20 June, 2007. **(b)** Slight ABB scattered in northern China during 21–30 June, 2007.

ACPD
10, 10589–10623, 2010

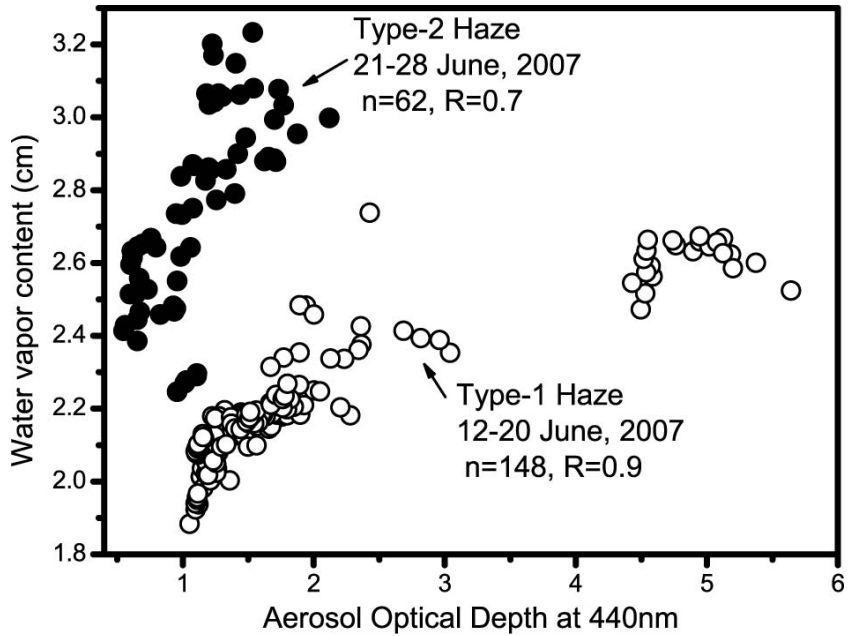

Fig. 9. Correlation between the aerosol optical depth at 440 nm and water vapor content during type-1 haze from 12–20 June and type-2 haze from 21 to 28 June, 2007 (http://aeronet.gsfc.nasa.gov/).

ACPD
10, 10589–10623, 2010

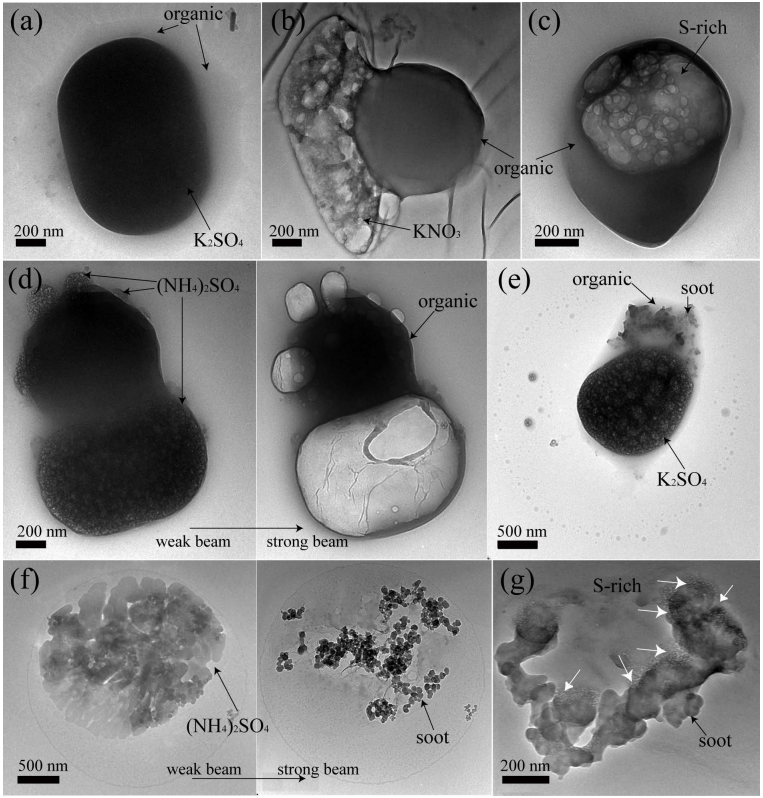

Fig. 10. Mixtures of organic, K-rich, S-rich, and soot. **(a)** K_2SO_4 with organic coating **(b)** KNO_3 coagulated with organic particle **(c)** S-rich particle (unidentified by SAED) mixed within organic particle **(d)** organic particle coagulated with $(NH_4)_2SO_4$ **(e)** Soot with organic coating coalesced with K_2SO_4. **(f)** Soot with $(NH_4)_2SO_4$ coating **(g)** soot coated by S-rich particles (unidentified by SAED).

ACPD
10, 10589–10623, 2010